

An *Escherichia coli* Mutant Quinol:Fumarate Reductase Contains an EPR-detectable Semiquinone Stabilized at the Proximal Quinone-binding Site*

(Received for publication, February 19, 1999, and in revised form, June 17, 1999)

Cecilia Hägerhäll[†], Sergey Magnitsky[‡], Vladimir D. Sled[‡], Imke Schröder[¶],
Robert P. Gunsalus^{||}, Gary Cecchini^{**††}, and Tomoko Ohnishi^{‡‡§§}

From the [†]Department of Biochemistry and Biophysics, University of Pennsylvania, Philadelphia, Pennsylvania 19104, the ^{||}Department of Microbiology and Molecular Genetics, University of California, Los Angeles, California 90095, the ^{**}Molecular Biology Division, Veterans Affairs Medical Center, San Francisco, California 94121, and the ^{‡‡}Department of Biochemistry and Biophysics, University of California, San Francisco, California 94143

The EPR and thermodynamic properties of semiquinone (SQ) species stabilized by mammalian succinate:quinone reductase (SQR) *in situ* in the mitochondrial membrane and in the isolated enzyme have been well documented. The equivalent semiquinones in bacterial membranes have not yet been characterized, either in SQR or quinol:fumarate reductase (QFR) *in situ*. In this work, we describe an EPR-detectable QFR semiquinone using *Escherichia coli* mutant QFR (FrdC E29L) and the wild-type enzyme. The SQ exhibits a $g = 2.005$ signal with a peak-to-peak line width of ~ 1.1 milliteslas at 150 K, has a midpoint potential ($E_{m(\text{pH } 7.2)}$) of -56.6 mV, and has a stability constant of $\sim 1.2 \times 10^{-2}$ at pH 7.2. It shows extremely fast spin relaxation behavior with a $P_{1/2}$ value of $\gg 500$ milliwatts at 150 K, which closely resembles the previously described SQ species (SQ_s) in mitochondrial SQR. This SQ species seems to be present also in wild-type QFR, but its stability constant is much lower, and its signal intensity is near the EPR detection limit around neutral pH. In contrast to mammalian SQR, the membrane anchor of *E. coli* QFR lacks heme; thus, this prosthetic group can be excluded as a spin relaxation enhancer. The trinuclear iron-sulfur cluster FR3 in the $[3\text{Fe-4S}]^{1+}$ state is suggested as the dominant spin relaxation enhancer of the SQ_{FR} spins in this enzyme. *E. coli* QFR activity and the fast relaxing SQ species observed in the mutant enzyme are sensitive to the inhibitor 2-*n*-heptyl-4-hydroxyquinoline *N*-oxide (HQNO). In wild-type *E. coli* QFR, HQNO causes EPR spectral line shape perturbations of the iron-sulfur cluster FR3. Similar spectral line shape changes of FR3 are caused by the FrdC E29L mutation, without addition of HQNO. This indicates that the SQ and the inhibitor-binding sites are located in close proximity to the trinuclear iron-sulfur cluster FR3. The data further suggest that this site corresponds to the proximal quinone-binding site in *E. coli* QFR.

Succinate:quinone reductase (SQR)¹ and quinol:fumarate reductase (QFR) are structurally and functionally similar enzymes with an interesting evolution (1–3). They consist of two well conserved subunits protruding from the membrane. A larger flavoprotein subunit (denoted Fp) harbors the dicarboxylate-binding site and a covalently bound FAD cofactor; a smaller iron-sulfur protein subunit (denoted Ip) contains three distinct iron-sulfur clusters. The $[2\text{Fe-2S}]^{2+,1+}$, $[4\text{Fe-4S}]^{2+,1+}$, and $[3\text{Fe-4S}]^{1+,0}$ clusters are called S1 or FR1, S2 or FR2, and S3 or FR3 in SQR and QFR, respectively. The membrane anchor domain of the enzyme is more variable and may consist of one or two hydrophobic polypeptides (SdhC/FrdC and SdhD/FrdD) and contain zero, one, or two b hemes depending on the enzyme species. When two hemes are present, they are denoted heme b_H and heme b_L. The primary sequence similarity is also much lower in this part of the enzyme. Nevertheless, accumulated evidence indicates that the membrane anchors have a conserved general structure (3, 4). One exception is a group of SQRs lacking the membrane domain and instead containing two different, more or less hydrophilic subunits (5).

The membrane-bound enzymes catalyze the oxidation of succinate or the reduction of fumarate in the bacterial cytoplasm or mitochondrial matrix and the reduction or oxidation of quinone/quinol in the membrane. It should be emphasized that when provided with suitable substrates *in vitro*, SQRs and QFRs generally can carry out both reactions; however, *in vivo*, they serve separate physiological functions. Thus, organisms capable of both aerobic and anaerobic life contain genes encoding both enzymes that are expressed during different growth conditions. There are three functionally distinct classes of SQR/QFR defined by the type of quinones that they use as electron acceptors/donors. Class 1 SQRs donate electrons to a quinone with a higher redox midpoint potential (E_m) such as ubiquinone, whereas Class 2 QFRs and Class 3 SQRs use a quinone with a lower E_m such as menaquinone (3). How the directionality of the enzyme reaction is achieved *in vivo* is not well understood, particularly for the Class 3 enzymes, but it is clear that the E_m values of the iron-sulfur clusters are differently tuned in the enzymes of a different functional class.

The presence of two quinone-binding sites on the membrane anchor, located toward opposite sides of the membrane, has been demonstrated in SQR/QFR enzymes by various methods.

* This work was supported in part by National Science Foundation Grants MCB-9418694 (to T. O.) and MCB-9728778 (to G. C.), the Department of Veterans Affairs (to G. C.), and National Institutes of Health Grant HL-16251 (to G. C. and I. S.). The costs of publication of this article were defrayed in part by the payment of page charges. This article must therefore be hereby marked "advertisement" in accordance with 18 U.S.C. Section 1734 solely to indicate this fact.

[†] This work is dedicated to the memory of Vladimir D. Sled.

[‡] Supported by National Science Foundation Grant MCB-9418694 during work carried out in the laboratory of T. O. Present address: Dept. of Biochemistry, Lund University, P. O. Box 124, 22100 Lund, Sweden.

[¶] These two authors contributed equally to this work.

^{§§} To whom correspondence should be addressed. Tel.: 215-898-8024; Fax: 215-573-3748; E-mail: Ohnishi@mail.med.upenn.edu.

¹ The abbreviations used are: SQR, succinate:quinone reductase; QFR, quinol:fumarate reductase; Q, ubiquinone; TTFA, 2-thenoyl-trifluoroacetone; HQNO, 2-*n*-heptyl-4-hydroxyquinoline *N*-oxide; SQ, semiquinone; QH₂, quinol; BisTris, 2-[bis(2-hydroxyethyl)-amino]-2-(hydroxymethyl)-propane-1,3-diol; mW, milliwatt(s); mT, millitesla(s).

Both membrane anchor polypeptides of *Bos taurus* SQR were photolabeled with [³H]arylazoquinone derivatives (6). In subsequent labeling studies using the same enzyme, two peptide regions, one in SdhC and the other in SdhD, were assigned as quinone-binding sites (7, 8). Recently, the N-terminal part of SdhC from *Escherichia coli* SQR was photoaffinity-labeled with a [³H]azoquinone analogue (9). Mutagenesis studies of the *E. coli* QFR membrane anchor polypeptides also outlined two quinone-binding regions (10) that overlap both with peptide stretches indicated in the bovine enzyme and with the stretch implied in bacterial SQR (see Fig. 1). This corroborates the structural similarity between the heme-less and the heme-containing membrane anchors. Apparently, extensive sequence variability is tolerated at the quinone-binding sites, but their location in the protein is nevertheless conserved. There is a quinone-binding region formed by amino acid residues from SdhCD/FrdCD located near the bacterial cytoplasmic or mitochondrial matrix side of the membrane. This region is referred to as Q-proximal (previously denoted Q_B), whereas an additional quinone-binding area located farther from the Fp and Ip subunits and near the other side of the membrane is termed Q-distal (or Q_A).

There are a number of inhibitors that interfere with the interaction of SQR/QFR with quinones. The most well known are 2-thenoyltrifluoroacetone (TTFA), 3-methylcarboxin, and 2-*n*-heptyl-4-hydroxyquinoline *N*-oxide (HQNO). Sensitivity to these inhibitors varies among species and SQR/QFR enzyme types. The two former compounds exhibit some structural similarity and are specific inhibitors (11, 12), whereas HQNO also inhibits various other enzymes interacting with quinones (13). Studies with resistant mutants of *Ustilago maydis* (14) and *Paracoccus denitrificans* (15) indicate that the carboxin-binding site overlaps with Q-proximal and that amino acids from both Ip (in fact, a residue within the cluster S3 ligation motif) and SdhD contribute to carboxin binding. Close proximity of S3 and the inhibitor-binding site is also apparent from the E_m shift of cluster S3 in pigeon heart submitochondrial particles (16) and bovine heart submitochondrial particles (17) caused by TTFA.

E. coli QFR and *Bacillus subtilis* SQR, both of which use menaquinone as an electron donor/acceptor, are not sensitive to carboxins or to TTFA, but are sensitive to HQNO (with apparent K_i values of 0.2 and 0.4 μ M, respectively (18); the former at pH 7.8 and the latter at pH 7.5).² Both studies show that the apparent K_i increases with increasing pH. In *B. subtilis* SQR as well as in isolated SdhC polypeptide, HQNO binding causes a shift in the EPR spectrum line shape and induces a shift in the E_m of heme b_L by about -60 mV, without affecting the heme b_H properties (19).³ This demonstrates that the HQNO-binding site in *B. subtilis* SQR is located in the vicinity of heme b_L, *i.e.* that it corresponds to Q-distal. It has also been shown that HQNO elicits a significant change in the EPR line shape of *E. coli* FR3, indicating the close proximity of the quinone-binding site and iron-sulfur cluster (20). Such EPR line shape changes were not detected in the *B. subtilis* enzyme (21, 22) in the presence of HQNO.

In mammalian mitochondria, multiple EPR signals at $g = 2.04$, 1.99, and 1.96 arising from spin-spin interactions were observed at temperatures <15 K (23). These spin-coupled split signals were absent in ubiquinone-depleted membranes and reappeared in ubiquinone-replenished membranes, indicating that one of the interacting partners was a semiquinone (SQ). Spectral simulations suggested a semiquinone (either semiqui-

TABLE I
Stability constants of different semiquinone species functioning as a converter in $n = 1 \leftrightarrow n = 2$ electron transfer processes in the respiratory chain compared with species functioning solely as $n = 2$ components

SQ species	K_S	E_m	pH
mV			
Converters of $n = 1 \leftrightarrow n = 2$ e ⁻ transfer processes			
<i>B. taurus</i> SMP ^a	SQ _s ⁻	10	+110 7.4
<i>E. coli</i> Frd C E29L membrane	SQ _{FR} ⁻	1.2×10^{-2}	-57 7.2
<i>B. taurus</i> SMP	SQ _i ⁻	5×10^{-2}	+80~+100 7.0
<i>R. spheroides</i> chromatophore	SQ _i ⁻	4×10^{-2}	+150 8.0
<i>B. taurus</i> bc ₁ complex	SQ _i ⁻	1×10^{-2}	+90 7.0
<i>R. capsulatus</i> chromatophore	SQ _i ⁻	1×10^{-4}	+150 7.0
$n = 2$ e ⁻ transfer processes			
Q pool		10^{-10}	+90 7.0
<i>R. capsulatus</i> chromatophore	SQ _{OS}	10^{-14}	+80 7.0
<i>R. capsulatus</i> chromatophore	SQ _{OW}	10^{-11}	+80 7.0

^a SMP, submitochondrial particles.

none or flavosemiquinone) spin-spin interaction overlapped with the cluster S3 signal (23). If the spin-coupled split signals were assumed to arise only from dipole-dipole interaction, the distance between the interacting spins was estimated to <7.7 Å (23). Subsequently, Ingledew and Ohnishi (16) and Salerno and Ohnishi (17) showed that these split signals arise from a semiquinone anion (Q_i⁻Q_s⁻) pair, based on detailed EPR and thermodynamic analysis of the rapidly relaxing Q_s⁻ $g = 2.00$ signal and the spin-coupled split signals. Both Q_s⁻ and the Q⁻Q⁻ pair are sensitive to the SQR-specific inhibitors carboxin and TTFA. The spin-coupled Q⁻ pair have similar E_m values: E_{m1} (Q⁻/Q) and E_{m2} (QH₂/Q⁻) = 140 and 80 mV, respectively, which correspond to a stability constant (K_S) of 10. This is many orders of magnitude greater than the K_S of the quinone pool, indicating a preferential binding of Q⁻ relative to Q and QH₂ (Table I). Similar spin-spin interaction signals have been observed in mitochondria from various plants (24) and the fungus *Neurospora crassa* (25). Neither semiquinone nor the spin-coupled split EPR signals have previously been directly demonstrated in bacterial SQR and QFR enzymes, although recent results based on spectral simulations suggest the presence of a similar semiquinone pair in *P. denitrificans* SQR (26).

In this work, we describe an EPR-detectable thermodynamically stabilized semiquinone in *E. coli* QFR using an FrdC E29L mutant (10). The semiquinone is sensitive to HQNO and demonstrates extremely fast spin relaxation behavior, similar to the previously described Q_s⁻ $g = 2.00$ signal of mitochondrial SQR. Furthermore, we demonstrate that in contrast to *B. subtilis* SQR, in *E. coli* QFR, HQNO interacts with the proximal quinone-binding site. The SQ species is also found in wild-type QFR, but has a much lower K_S and is detectable only in the higher pH range.

MATERIALS AND METHODS

The *E. coli* strains, plasmids, and phage used in this study have been previously described (10). To obtain higher expression levels of the mutant forms of QFR discussed in this work, it was necessary to reconstruct the *frdC* mutations that had been previously made using a low copy number, *i.e.* two-plasmid expression system (10). Thus, site-directed mutagenesis was performed using the *in vitro* mutagenesis system from Bio-Rad based on the method developed by Kunkel (27) and Kunkel *et al.* (28) using single-stranded M13 DNA containing the *frdCD* genes as template. Oligonucleotides were designed and synthesized on a Biosearch Model 8700 nucleic acid synthesizer to change the nucleotides in *frdC* encoding Glu-29, His-82, and Trp-86 to codons for the selected amino acid substitutions. The mutations were confirmed by DNA sequence analysis using the dideoxy termination procedure (29) and a Ladderman DNA sequencing kit (Panvera Corp., Madison, WI). Following mutagenesis, the 1070-base pair *DraIII-XhoI* fragment con-

² Maklashina, E., and Cecchini, G. (1999) *Arch. Biochem. Biophys.*, in press.

³ V. Borisov, I. Smirnova, C. Hägerhäll, A. Konstantinov, and L. Hederstedt, manuscript in preparation.

taining the desired mutation was cloned into plasmid pH3 (30) to restore the complete *frdABCD* operon with the desired mutation. Plasmids containing the mutations were then transformed into strain DW35 (Δ *frdABCD* *sdhC::kan*) (10) to give high level expression of membrane-bound QFR. *E. coli* strain DW35 cells containing pH3 plasmids encoding wild-type or mutant forms of QFR were grown anaerobically on glucose/fumarate medium as described previously (31). Cells were harvested in the early stationary phase of growth, and the membrane fraction was prepared from a French pressure cell lysate as described previously (32).

Redox titrations were performed at room temperature (25 °C) in an airtight vessel flushed with oxygen-free argon and equipped with a magnetic stirring device, an Ag/AgCl-platinum combination electrode, and a pH electrode essentially as described (33). The redox potential of the reference electrode was calibrated *versus* a saturated solution of quinhydrone (285 mV *versus* normal hydrogen electrode at pH 7). The following redox mediators, dissolved in H₂O (indigo dyes) or Me₂SO, were used at 25–50 μ M final concentrations: 5,5'-indigodisulfonate (–125 mV), 5,5',7-indigotrisulfonate (–80 mV), 5,5',7,7'-indigotetrasulfonate (–46 mV), 2-hydroxy-1,4-naphthoquinone (–152 mV), 1,4-naphthoquinone-2-sulfonate (+113 mV), 1,4-naphthoquinone (+50 mV), and duroquinone (+7 mV). In total, <0.15% Me₂SO was added. Reductive titrations were carried out by stepwise addition of an anaerobic sodium dithionite solution, and samples were transferred anaerobically to EPR tubes, frozen in a cold mixture of isopentane/methylcyclohexane (5:1) at about –80 °C, and stored in liquid nitrogen until EPR analyses. The relative concentration of the intermediate SQ form (y) as a function of the ambient redox potential (E_h) is described by Equation 1,

$$y = \frac{1}{1 + 10^{(E_h - E_m^{1/0})/59} + 10^{(E_m^{2/1} - E_h)/59}} \quad (\text{Eq. 1})$$

where $E_m^{1/0}$ and $E_m^{2/1}$ are E_m values of two consecutive 1-electron transfer steps. Alternatively, membranes were poised at different ambient E_h values using the substrate couple succinate/fumarate (1:1) at a 20 mM total concentration under argon by changing the ambient pH in the absence of redox mediator dyes. The same titration vessel and setup as for the potentiometric titration were used. The pH, initially 6.0, was gradually altered by small additions of 5 M NaOH and, when approaching a pH of ~9.5, was followed by similar additions of 5 M HCl. EPR samples were taken 5 min after each addition to ensure equilibrium and were frozen and stored as before. In both cases, the *E. coli* membranes were suspended in 50 mM BisTris and 3 mM EDTA (pH as indicated) at 25 mg/ml membrane protein. At this protein concentration, the membranes routinely contained $32 \pm 5 \mu$ M QFR, based on spin quantitation of the iron-sulfur cluster Fr1. HQNO, when present, was added at ~5:1 stoichiometry (150 μ M). Protein was determined as described (34). Spin quantitation under non-power-saturated conditions was performed as described (35) using 0.5 mM CuEDTA as a standard. EPR spectra were recorded using an X-band Bruker ESP-300E EPR spectrometer equipped with an Oxford Instruments ESR-9 helium flow cryostat. Other EPR conditions were as indicated in the figure legends. The power saturation data were analyzed by computer fitting to Equation 2,

$$A = \sum_{i=1}^n A_i = \sum_{i=1}^n C_i \frac{\sqrt{P}}{(1 + P/P_{50(i)})^{0.5b_i}} \quad (\text{Eq. 2})$$

where A_i is the amplitude of the i th-type free radical, C_i is a coefficient for the actual content of the i th-type free radical in the sample, $P_{50(i)}$ is the half-saturation microwave power, b_i is the “inhomogeneity parameter,” and n is numbers of components (36, 37). Simulation of the power saturation and redox titration curves was performed using the software Origin (MicroCal Software, Inc.) using the Marquardt-Lovenberg algorithm and simplex method for nonlinear least-square fitting.

RESULTS

The previous EPR studies using mammalian SQR showed that semiquinone signals were more readily detected in submitochondrial particles compared with more resolved preparations or the isolated enzyme (38–40). In mitochondrial and bacterial inner membranes, other free radical species are also present. SQR-specific inhibitors such as carboxin and TTFA can be used in the mammalian experimental system, but for *E. coli* QFR, we have no specific inhibitors available. Thus, we compared redox titrations of membranes from *E. coli* strain

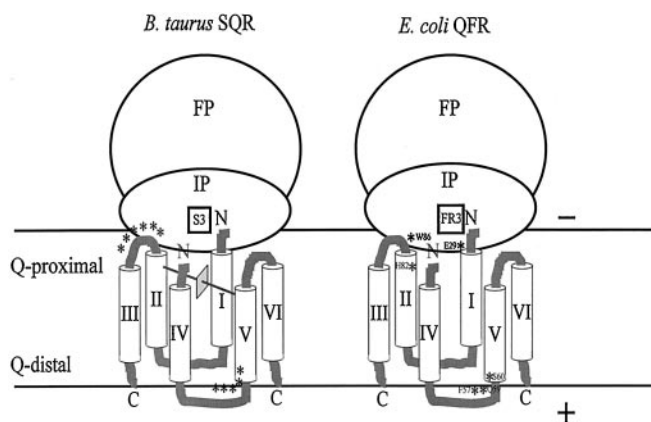


FIG. 1. Structural models of the SQR and QFR membrane anchor subunits (adapted from Ref. 4 as discussed under “Discussion”) with the iron-sulfur cluster S3/FR3, quinone-photolabeled areas (7–9), and point mutations (10) (indicated by *). The SdhC/FrdC polypeptides contain transmembrane helices labeled I, II, and III; and SdhD/FrdD contain helices labeled IV, V, and VI. SQR contains histidine axial ligands for heme b on helices II and V as indicated, whereas *E. coli* QFR lacks heme.

DW35, deleted of both the QFR- and SQR-encoding operons (10), with membranes from DW35 expressing wild-type or mutant QFR. The overexpression of QFR also facilitated detection of QFR-bound semiquinone *versus* other unrelated free radicals in the system. In this study, attention was focused on the proximal quinone-binding site in QFR; and thus, we selected three of the most promising of the previously generated membrane anchor mutants predicted to reside in this area, *i.e.* FrdC E29L, H82R, and W86R (10) (Fig. 1).

EPR analyses of cytoplasmic membranes of *E. coli*, poised by conventional potentiometric redox titrations, showed that a weak SQ free radical $g = 2.00$ signal was present in both DW35 (QFR- and SQR-deleted) membranes and DW35 membranes containing wild-type QFR. The SQ species showed E_m values of approximately –30 and –50 mV, respectively, with about the same spin concentration/mg of membrane protein (data not shown). Both semiquinone signals were very slow relaxing; and in addition, neither signal was affected by HQNO.

In contrast, membranes from FrdC E29L mutant QFR exhibited another SQ free radical species with much faster spin relaxation behavior ($P_{1/2} \gg 500$ mW)⁴ at 123 K similar to the SQ_s species of bovine heart SQR, in addition to the slow relaxing SQ species. Fig. 2 shows a potentiometric titration curve of the semiquinone $g = 2.005$ signal in the cytoplasmic membrane of the FrdC E29L mutant. SQ spectra were recorded at 5-mW microwave power to minimize the overlapping slow relaxing SQ signals. Curve-fitting computer analysis provided E_{m1} (SQ/Q) = –112 mV and E_{m2} (QH₂/SQ) = +1.2 mV, which correspond to $E_{m(\text{pH } 7.2)} = -56.6$ mV and a SQ stability constant (K_S) of 1.2×10^{-2} . Both first and second electron transfer steps were assumed as $n = 1$ steps. The E_m value corresponds to the peak redox potential of the bell-shaped titration curve, which equals the average of E_{m1} and E_{m2} . This SQ signal was quenched by HQNO. The SQ $g = 2.005$ spectra of the sample poised near the titration peak is shown below in Fig. 4.

The amplitude of the SQ signal in FrdC E29L mutant membranes at a sample temperature of 150 K was plotted as a function of microwave power in Fig. 3A. The observed biphasic saturation curve was resolved into two distinct components

⁴ Commercial X-band EPR spectrometers can measure to a maximum of only a 200-mW level. Although we obtained very high $P_{1/2}$ values such as >500 mW by computer fitting, it means that the sample has extremely fast spin relaxation from a practical point of view.

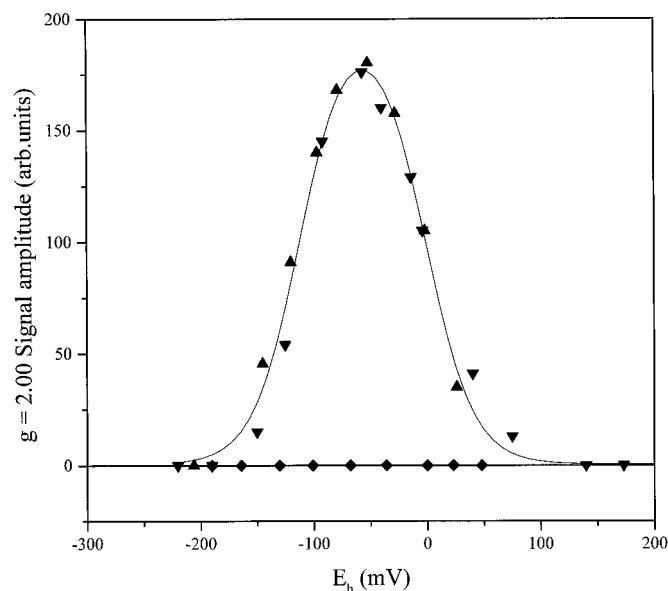


FIG. 2. Potentiometric titration curves of the semiquinone $g = 2.00$ signal amplitude as a function of E_h , analyzed in the presence of the redox mediator dyes at pH 7.2, in *E. coli* E29L mutant QFR (data points from two independent titrations are shown (▲ and ▼)) and in the presence of $150 \mu\text{M}$ HQNO (◆). The bell-shaped continuous line represents a theoretical simulated titration curve with E_{m1} and E_{m2} values of -112 and $+1.2$ mV, respectively, corresponding to an E_m of -56.6 mV. The E29L mutant membrane preparation ($30 \mu\text{M}$ QFR) was titrated at 25 mg/ml protein. The titration was conducted under anaerobic conditions as described under "Materials and Methods." EPR measurements of semiquinone signals were conducted using a Varian E109 spectrometer and a Johnson Foundation cold nitrogen gas flow system under the following conditions: sample temperature, 123 K; microwave power, 5 mW; modulation amplitude, 1.0 mT; modulation frequency, 100 kHz; time constant, 0.128 s; scanning field width, 40 mT; scanning time, 4 min; and microwave frequency, 9.190 GHz. *arb. units*, arbitrary units.

with $P_{1/2}$ values of 0.095 and 788 mW, respectively. At 1 - and 10 -mW microwave power levels, ~ 90 and $\sim 95\%$ of the spectral contribution arise from signals of the extremely rapidly relaxing SQ component, respectively. Shown in Fig. 3B are the power saturation profiles of the wild-type enzyme compared with the two remaining mutant QFR species, FrdC H82R and W86R. These samples show $P_{1/2}$ values of 0.095 , 0.12 , and 0.13 mW, respectively. Only the fast relaxing ($P_{1/2} = 788$ mW component)⁴ SQ species of FrdC E29L is sensitive to low concentrations of HQNO (HQNO/QFR = $5:1$). The EPR signal of the low $P_{1/2}$ SQ species of the wild-type enzyme and the FrdC H82R and W86R QFR mutants is insensitive to HQNO at this concentration range. The slow relaxing SQ signal is almost completely power-saturated under the EPR condition used in Fig. 2.

The maximal amplitudes of both the fast and slow relaxing SQ signals were increased by changing the ambient pH of the potentiometric titrations from 7 to 9 , suggesting that these semiquinone species are mostly in an anionic form (Q^-) within this pH range. The semiquinone EPR spectra of E29L mutant QFR poised potentiometrically near the titration peak at pH 7.2 and 9.0 are shown in Fig. 4. The signal amplitude of SQ at pH 9.0 is higher than at pH 7.2 , indicating that SQ is in an anionic form (Q^-) in this pH range. Both spectra exhibit an ~ 1.1 -mT peak-to-peak line width with a gaussian-type EPR line shape. Around pH 7 , the SQ signal was almost completely quenched by HQNO at a concentration ratio of $5:1$ molar excess to QFR, whereas at pH 9 , only $\sim 80\%$ of the signal was quenched (HQNO is known to be a less effective inhibitor at higher pH). We concluded that the fast relaxing SQ radical in the FrdC E29L mutant is QFR-associated and that the SQ state

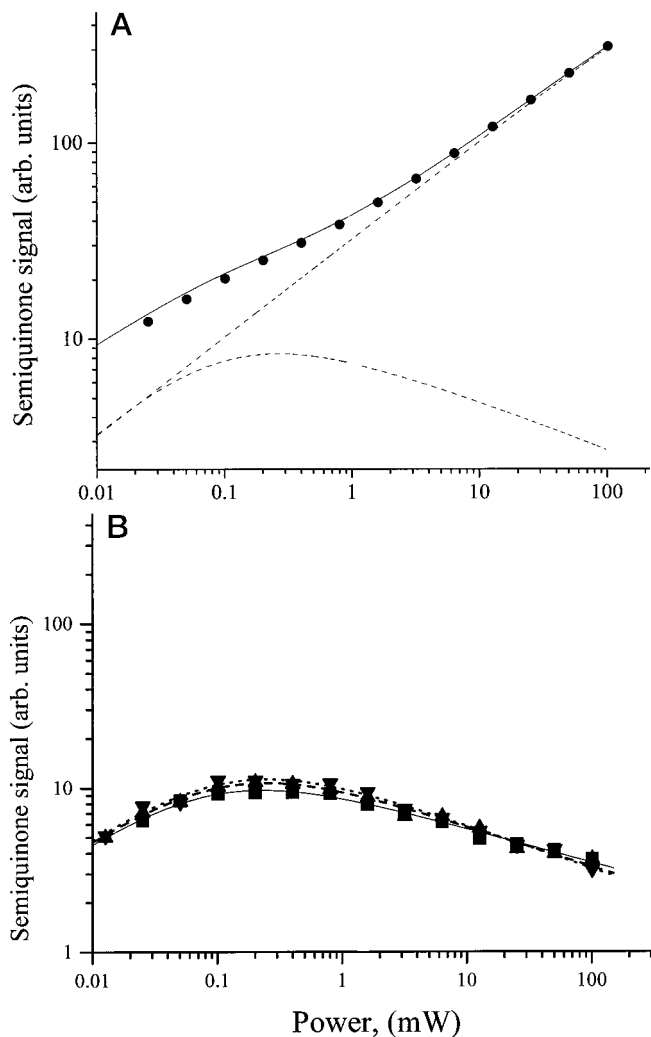


FIG. 3. Power saturation profiles of semiquinone signals poised by potentiometric redox titration at pH 7.5 and recorded at 150 K. **A**, the saturation curve (●) of the SQ free radical spins in QFR of the FrdC E29L mutant membranes was resolved into two components by computer fitting as described under "Materials and Methods." The best fit theoretical curve was drawn through the experimental points corresponding to the sum of two power saturation curves with $P_{1/2}$ values of 788 and 0.095 mW. **B**, presented are saturation behaviors of SQ signals in membranes containing wild-type QFR (■; $P_{1/2} = 0.095$ mW) and two other mutant membranes, H82R (▲; $P_{1/2} = 0.12$ mW) and W86R (▼; $P_{1/2} = 0.13$ mW). DW35 membranes lacking QFR and SQR also exhibit only the slow relaxing component (not shown). *arb. units*, arbitrary units.

is more strongly bound to QFR than the oxidized or fully reduced states. In contrast to mitochondrial SQR *in situ*, no spin-coupled split signals indicative of a spin-coupled SQ pair were detected in *E. coli* QFR over a wide range of low temperatures.

Glu-29 in FrdC was among the first residues in the *E. coli* QFR membrane anchor to be implicated in interactions with quinones. This residue was proposed to facilitate protonation/deprotonation of the quinone (10), in analogy with a glutamate residue in the photosynthetic reaction center Q_B (41). It should also be noted that Glu-29 from FrdC is located in the vicinity of the peptide stretch recently labeled with [^3H]azidoquinone in *E. coli* SQR (9) (see Fig. 1). In the structural model of the membrane anchor, Glu-29 is predicted to be located at or close to Q-proximal and thus near to the iron-sulfur cluster FR3 (Fig. 1). Fig. 5A shows the EPR spectrum of the FR3 [$^3\text{Fe-4S}$] $^{1+}$ ($1+,0$) cluster in wild-type membranes in the oxidized state. Addition of the inhibitor HQNO to wild-type membranes altered the EPR spectral line shape in the central region of the FR3 spec-

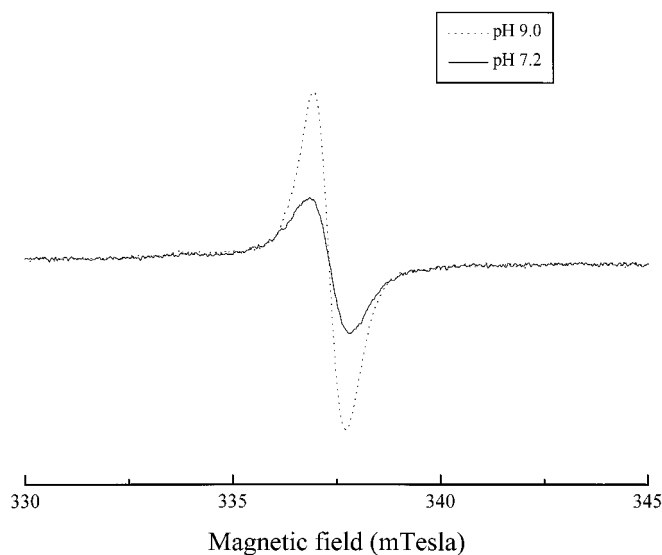


FIG. 4. EPR spectra of semiquinones in *E. coli* mutant QFR (FrdC E29L). The redox state was poised potentiometrically close to the maximum of the bell-shaped titration curves at pH 7.2 (—) and at pH 9.0 (····). E_h values were -16 and -41 mV, respectively. EPR conditions were as follows: modulation amplitude, 0.63 mT; sample temperature, 150 K; microwave power, 1.6 mW; time constant, 81.9 ms; and scanning rate, 167.8 s.

trum (Fig. 5B) as described (20). EPR line shape perturbation of the FR3 spectrum in the E29L mutant is similar to that seen when the wild-type QFR FR3 spectrum is perturbed by HQNO (Fig. 5C). No further FR3 line shape changes occurred after HQNO addition to FrdC E29L mutant QFR (data not shown). These observations provide evidence that FR3 is in close proximity to the Q-proximal binding site and agree with the observations of Rothery and Weiner (20). Furthermore, the location of the observed semiquinone in the vicinity of FR3 is consistent with the position of Glu-29 of FrdC in the structural model (Fig. 1) (3, 4) of the QFR membrane anchor.

To circumvent the interference with intensified $g = 2.00$ signals from the redox mediator dyes in the high pH range, we poised QFR under anaerobic conditions using the substrate couple succinate/fumarate at a 1:1 ratio at a total concentration of 20 mM, which is 3 orders of magnitude higher than the QFR concentration (Fig. 6). The ambient redox potential (E_h) was altered by gradually changing the pH from <6.5 to >9.5 by addition of small aliquots of alkali or acid, using the pH dependence (-60 mV/pH unit) of the succinate/fumarate redox couple. These experimental conditions were non-deleterious to QFR since the sequential oxidative and reductive titrations could be performed with reasonable reproducibility. As presented in Fig. 6, SQ peak-to-peak signal amplitude as a function of the ambient pH showed a biphasic curve, increasing SQ signal amplitude with increasing pH. Unfortunately, DW35 (QFR- and SQR-deleted) membranes cannot be used as a control in this system. Nevertheless, we observed biphasic power saturation profiles of the SQ species with extremely high ($>>500$ mW) and low ($0.05 < P_{1/2} < 0.3$ mW) $P_{1/2}$ values in the E29L mutant membrane, similar to those observed during potentiometric titration. The inhibitory effect of HQNO decreases with increasing pH in the range above pH 8.5. Although the SQ signal intensity is much lower in the wild-type membranes, the presence of an HQNO-sensitive SQ signal is clearly discernible at a pH range higher than 9.0.

In Fig. 7, the EPR spectra of FR3 poised at redox potentials of $+15.6$, -40.2 , and -94.8 mV are presented, which correspond to pH values of 7.2, 8.2, and 9.1, respectively. Since the E_m value of the trinuclear iron-sulfur cluster FR3 in both

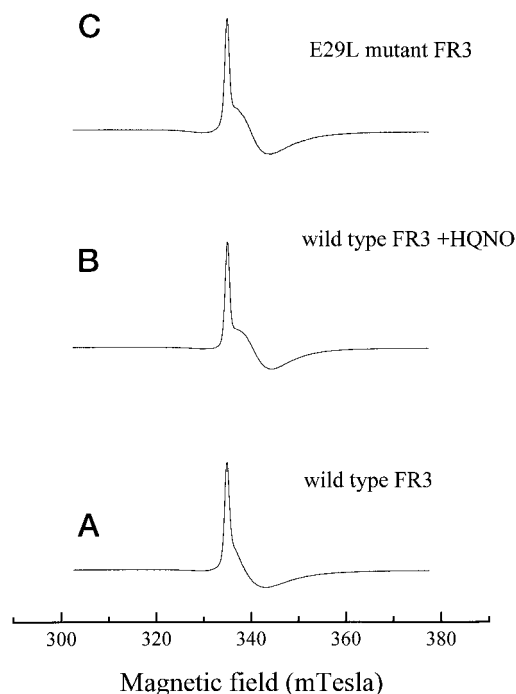


FIG. 5. EPR spectra of the oxidized trinuclear iron-sulfur cluster FR3 in wild-type QFR (A), in the presence of a 5:1 molar excess HQNO (B), and in E29L mutant QFR (C). The latter did not exhibit further changes upon HQNO addition. EPR conditions were as follows: microwave frequency, 9.4455 GHz; modulation amplitude, 1.0 mT; microwave power, 2 mW; time constant, 0.164 s; and scanning rate, 0.6 mT/s. Spectra were recorded at 7 K.

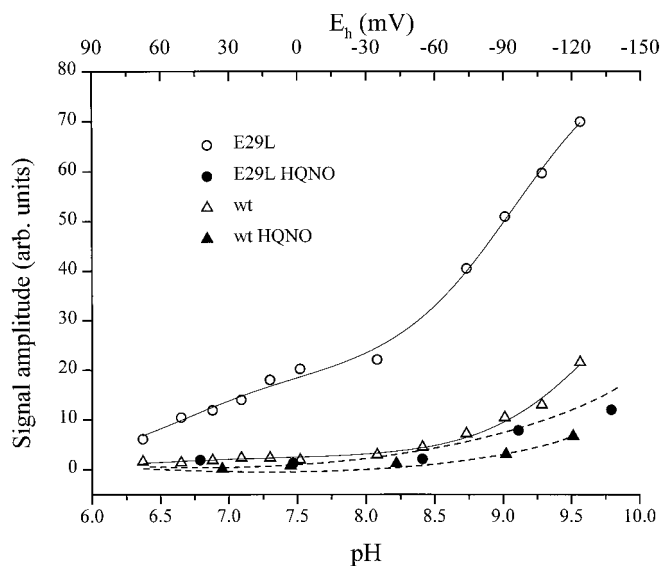


FIG. 6. pH titration using the succinate/fumarate couple recorded at 100 K and 0.5 mW. \circ , membranes containing E29L mutant QFR; Δ , membranes containing wild-type QFR (wt); \bullet and \blacktriangle , the same titrations in the presence of 150 μ M (5:1 molar excess) HQNO, respectively. The membranes contained 30 μ M QFR, 25 mg/ml protein in 50 mM BisTris, 1 mM EDTA, 10 mM succinate, and 10 mM fumarate. The E_h of the succinate/fumarate couple is based on the E_{m7} of $+30$ mV and the normal pH dependence of -60 mV/pH unit. *arb. units*, arbitrary units.

wild-type and E29L mutant QFR is in the range of approximately -70 to -50 mV and is pH-independent, the relative concentration of the oxidized $[3\text{Fe-4S}]^{1+}$ cluster FR3 is decreased when the ambient pH of the succinate/fumarate redox couple is increased (Table II). Resolution of the biphasic power saturation curves showed that the ratio of high $P_{1/2}$ SQ versus

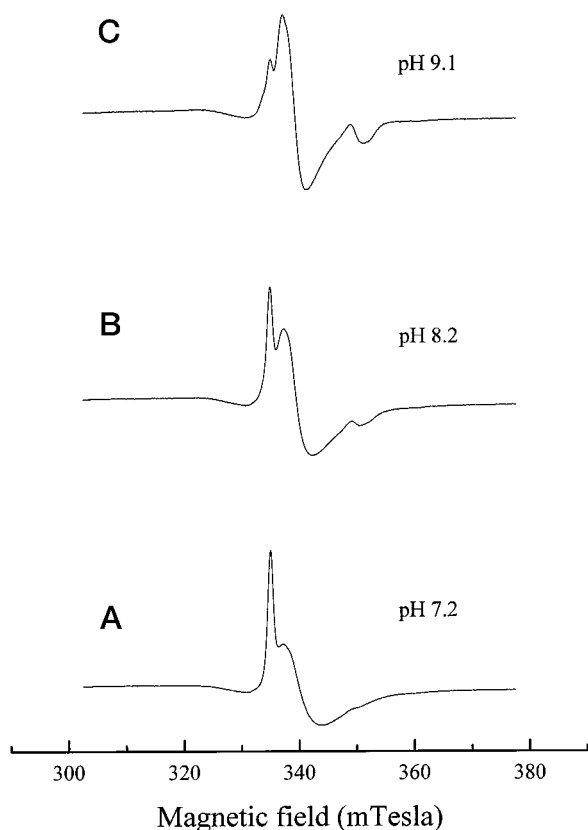


FIG. 7. EPR spectra of the FR3 cluster in E29L mutant QFR poised with 20 mM succinate/fumarate buffer at three different pH values. EPR conditions were as described in the legend to Fig. 5.

low $P_{1/2}$ SQ varied as 2.8, 2.3, and 1.2 in parallel with pH changes of 7.2, 8.2, and 9.1, respectively. Concomitantly, the concentration of the oxidized FR3 amplitude decreased as 3.9, 2.4, and 1.0, respectively. This strongly suggests that the trinuclear cluster FR3 in the oxidized state ($[3\text{Fe-4S}]^{1+}$ spin 1/2 ground state) seems to be a more effective spin relaxant of the QFR SQ spins than the reduced state $[3\text{Fe-4S}]^0$ cluster FR3 (spin 2 ground state). It should be pointed out that we estimated the relative concentrations of the FR3 cluster ($[3\text{Fe-4S}]_{\text{FR3}}^{1+}$) based on the amplitude of the 2.02 g_z peak, which is consistent with the calculated redox change in the E_m and E_h values of the three selected EPR samples of the titration in Fig. 6. However, it is discernible that the central EPR spectral line shape of the FR3 cluster could be significantly altered during the titration from curve A to C (Fig. 7). Detailed computer simulations are needed for more rigorous analysis of the correlation suggested above.

The SQ spectra of *E. coli* FrdC E29L membranes at three different pH values are presented in Fig. 8. Notably, the SQ spectral line shape of the succinate/fumarate poised system is more a Lorentzian-type than that obtained by potentiometric titration, although the peak-to-peak width is the same. The SQ signal intensity increased with increasing pH in the same manner as the potentiometrically poised system (Fig. 4). This indicates that the SQ species in *E. coli* QFR is in the anionic form (Q^-) in the pH 7–9 range.

DISCUSSION

In this work, we have shown that an *E. coli* mutant (FrdC E29L) QFR contains an EPR-detectable semiquinone thermodynamically more stable than the wild-type enzyme. Semiquinone species associated with succinate:quinone oxidoreductase

TABLE II

Comparison of the relative concentrations of fast relaxing semiquinone spins of QFR and concentration of the trinuclear iron-sulfur cluster FR3 in the oxidized state versus in the reduced state

Power saturation parameters (P_{SO} values in milliwatts) of the SQ $g = 2.005$ signals of QFR at three pH values (Fig. 8) were analyzed as described in the legend to Fig. 3. Signal contributions from the extremely fast and slow relaxing spins were resolved by computer fit. Since the total spin concentrations of the FR3 cluster in these samples were the same, the relative concentration of the $[3\text{Fe-4S}]^{1+}$ state was estimated from the peak amplitude of $g_z = 2.02$.

pH	E_h	P_{SO} SQ-fast	Relative conc of SQ-fast	Relative conc of $[\text{FR3}]_{\text{ox}}$
9.1	-94.8	813	1.2	1.0
8.2	-40.2	982	2.3	2.4
7.2	+15.6	813	2.8	3.9

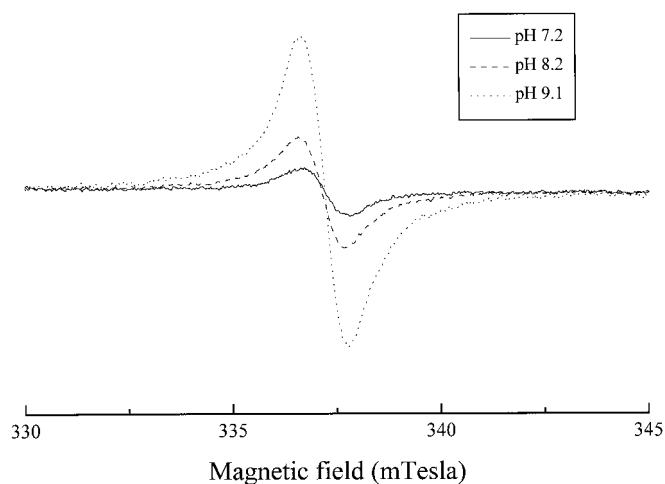


FIG. 8. Semiquinone signals in the same samples shown in Fig. 7, monitored at the sample temperature of 150 K, a microwave power of 1.6 mW, and a modulation amplitude of 0.63 mT. Other EPR conditions were as described in the legend to Fig. 4.

have previously been directly demonstrated only in eukaryotic organisms.⁵

Our results represent the first direct observation of a stabilized semiquinone in bacterial QFR. In both the previously described mammalian SQR and *E. coli* QFR, the observed semiquinone is apparently stabilized at the proximal quinone-binding site. The effect of quinone-binding site inhibitors on cluster S3 in mitochondria (16, 17) in combination with the location of mutations in other species giving resistance to the same inhibitors (14, 15) demonstrates this fact. In *E. coli* QFR, the effect of the E29L mutation on the EPR line shape of cluster FR3, similar to that observed in the wild-type enzyme in the presence of HQNO, in combination with the effect of HQNO on the E29L stabilized semiquinone is consistent with a closeness between the proximal quinone-binding site and the iron-sulfur cluster FR3. In addition, these data are consistent with the position of Glu-29 in the current structural model (3, 4) of the QFR membrane anchor. However, in bovine SQR and seemingly in *P. denitrificans* SQR (both Class 1 SQRs donating electrons to ubiquinone), the semiquinone is stabilized in the wild-type enzyme, whereas in *E. coli* QFR (oxidizing menaquinol), the semiquinone at the proximal site is not detected in the wild-type enzyme. However, an HQNO-sensitive SQ species was clearly detectable in the pH range of 9.0–9.5, although its signal intensity was equivalent to only 15–20% of the counter-

⁵ During the preparation of this manuscript, we learned that X. Yang and L. Yu have detected semiquinone signals from wild-type *E. coli* SQR *in situ* (L. Yu, personal communication).

part signal detectable in the E29L mutant (Fig. 6). In the catalytic reactions of SQRs/QFRs, it is known that semiquinones are necessary for the transition of the $n = 1 \leftrightarrow n = 2$ electron transfer steps. However, for the same functional role, a wide range of stability constants for semiquinones can be found in the literature with differences of several orders of magnitude depending on the preparation. Even larger differences are seen depending on the physiological function of certain quinone-binding site(s) (2, 3) (see Table I). The E29L mutant is in fact severely defective in both quinol oxidase and quinone reductase activities, and one may speculate that the proximal-Q site in *E. coli* QFR is meant to produce a thermodynamically relatively unstable semiquinone for its physiological $n = 1 \leftrightarrow n = 2$ converter function. Analogously, a decrease in enzyme activity was reported upon the stabilization of SQ_i in the case of an H271R mutant of cytochrome *b* in the *Rhodobacter capsulatus* chromatophore *bc*₁ complex (42, 43).

In a recent study by Ishii *et al.* (44), it was demonstrated that a glycine-to-glutamate mutation in the *Caenorhabditis elegans* SdhC subunit resulted in oxidative stress and premature aging in the nematode. Alignment of SdhC/FrdC subunits from various species places this glycine residue in the vicinity of Glu-29 in FrdC (4). As shown in this work, mutation of Glu-29 in *E. coli* QFR results in the stabilization and easier detection of SQ. Long-lived semiquinones are prone to react with oxygen. Thus, similar perturbation of the quinone-binding environment in *C. elegans* mutant SQR could be responsible for the increased oxidative stress and premature aging.

The semiquinone detected in E29L mutant QFR demonstrates extremely fast spin relaxation behavior, similar to that found for the SQR semiquinone from *B. taurus* mitochondria. In the latter case, it has been suggested that spin relaxation of the SQR semiquinone is enhanced by the very fast relaxing S3 spins in the oxidized ($S = 1/2$) spin state and/or by the heme spins of the membrane anchor cytochrome *b* (17, 39). Since QFR lacks heme, the spin interacting partner of the E29L semiquinone has to be the [3Fe-4S] cluster FR3. The E_m of the succinate/fumarate couple is pH-dependent (-60 mV/pH unit), whereas the E_m of the FR3 cluster is not. Thus, during the succinate/fumarate pH titrations shown, the iron-sulfur cluster FR3 is changed from oxidized at low pH to more reduced states at higher pH (Fig. 7). In the oxidized [3Fe-4S]¹⁺ state of the iron-sulfur cluster FR3, three high spin ($S = 5/2$) Fe³⁺ atoms are anti-ferromagnetically coupled to give an $S = 1/2$ ground state in the low temperature range; in this case, one unpaired valence electron is delocalized among three Fe³⁺ atoms. In the reduced ([3Fe-4S]⁰) state of the FR3 cluster, the overall system is in the $S = 2$ spin state, arising from antiferromagnetic interaction between a valence-delocalized Fe³⁺/Fe²⁺ pair ($S = 9/2$) and a valence-localized Fe³⁺ site ($S = 5/2$) (45). Although the FR3 cluster is paramagnetic in both the oxidized and reduced states, it is more efficient in relaxing the spin of the reduced cluster FR1 in the oxidized $S = 1/2$ form than in its reduced $S = 2$ spin state (1). As shown in Fig. 6 and Table I, spin relaxation of SQ in FrdC E29L mutant QFR is also more effectively enhanced by the oxidized $S = 1/2$ state FR3 than by the reduced $S = 2$ state FR3, as in the case of the Q_s⁻Q_s⁻ pair in mitochondrial SQR and the [2Fe-2S]_{S1} cluster in *Micrococcus luteus* SQR (46). The spin-coupled Q_s⁻Q_s⁻ split signals were not detected in *E. coli* E29L mutant QFR. Notably, in addition to mammalian mitochondria SQR, the spin-coupled Q_s semiquinone pair has been observed only in some green plant mitochondria (24) and in mitochondria from *N. crassa* (25). This may be due to the fact that EPR signals from an interacting semiquinone pair are much more sensitive to perturbations than a single semiquinone. If the two interacting semiquinones

function as independent electron (or proton) transfer components, the concentration of the interaction signals would be the square function of the individual semiquinone concentrations. A modest shift of ~ 40 mV in the E_m of one bound quinone relative to the other would cause an almost complete lack of signal (17). We cannot, however, exclude the possibility that in *E. coli* QFR, only a single quinone molecule exists at the Q-proximal domain rather than the interacting pair.⁶

In a previous study by Westenberg *et al.* (10), Glu-29 of FrdC was replaced by aspartate, lysine, or phenylalanine, in addition to the replacement by leucine (10). To understand more about the stabilization of this semiquinone in *E. coli* QFR, we will perform EPR and thermodynamic analysis of membranes from QFR FrdC mutants such as E29D, E29F, and E29R.

The location of the HQNO-binding site is also of interest. As mentioned in the Introduction, in *B. subtilis* SQR, HQNO binding induces a shift in the E_m of heme b_L of about -60 mV, but has no effect on the E_m of heme b_H (19), indicating that the HQNO-binding site in *B. subtilis* SQR corresponds to Q-distal. Furthermore, in *B. subtilis*, no effect of HQNO on the EPR properties or thermodynamic behavior of S3 was detected (21, 22), although a Q-proximal site is seemingly present in *B. subtilis* SQR (21, 22). In this study, it is clear that in *E. coli* QFR, the inhibitor HQNO interacts with the proximal quinone-binding site. We can thus conclude that HQNO binds to the opposite quinone-binding site in *E. coli* QFR versus that in *B. subtilis* SQR. This is particularly interesting in light of the reverse function and different directionality of these two enzymes, which both use menaquinone as the electron donor/acceptor.

Although HQNO is a potent inhibitor of QFR, it also inhibits other components in the respiratory chain. The Q_i site of the cytochrome *bc*₁ complex interacts with HQNO, and formate dehydrogenase and a number of quinol-oxidizing enzymes are HQNO-sensitive, including QH₂-nitrate reductase, the *o*- and *d*-type ubiquinol oxidases (47), and Me₂SO reductase. A recent paper describes the interaction of an engineered [3Fe-4S] cluster in Me₂SO reductase with HQNO (48), indicating the presence of a proximal HQNO-binding site also in this quinol-oxidizing enzyme, analogous to that in *E. coli* QFR. The structure of HQNO resembles a semi(naphtho)quinone. The apparent K_i values for HQNO of *B. subtilis* SQR and *E. coli* QFR increase with increasing pH, indicating that the deprotonated inhibitor is less efficient (18). Thus, one may speculate that HQNO binds to topographically different, but perhaps functionally similar sites in *E. coli* QFR and *B. subtilis* SQR.

Acknowledgment—T. O. thanks R. Lin for excellent general assistance in preparing this manuscript.

REFERENCES

- Ackrell, B. A. C., Johnson, M. K., Gunsalus, R. P., and Cecchini, G. (1992) in *Chemistry and Biochemistry of Flavoenzymes* (Müller, F., ed) Vol. III, pp. 229–297, CRC Press, Inc. Boca Raton, FL
- Hederstedt, L., and Ohnishi, T. (1992) in *Molecular Mechanisms in Bioenergetics* (Ernster, L., ed) pp. 163–198, Elsevier Science Publishers B. V., Amsterdam
- Hägerhäll, C. (1997) *Biochim. Biophys. Acta* **1320**, 107–141
- Hägerhäll, C., and Hederstedt, L. (1996) *FEBS Lett.* **389**, 25–31
- Janssen, S. G., S., Anemuller, S., and Moll, R. (1997) *J. Bacteriol.* **179**, 5560–5569
- Yu, C.-A., and Yu, L. (1982) *J. Biol. Chem.* **257**, 6127–6131
- Lee, G. Y., He, D.-Y., Yu, L., and Yu, C.-A. (1995) *J. Biol. Chem.* **270**, 6193–6198
- Shenoy, S. K., Yu, L., and Yu, C.-A. (1997) *J. Biol. Chem.* **272**, 17867–17872

⁶ After the original submission of this manuscript, the x-ray crystallographic structure of *E. coli* quinol:fumarate reductase at 3.3-Å resolution was completed (49). Our proposed proximity of FrdC Glu-29 to the Q-proximal site and detection of the spin-spin interaction between SQ-proximal and [3Fe-4S]_{FR3} are consistent with the determined center-to-center distances of ~ 4 –5 and 9–11 Å (49), respectively.

9. Yang, X., Yu, L., He, D., and Yu, C.-A. (1998) *J. Biol. Chem.* **273**, 31916–31923
10. Westenberg, D. J., Gunsalus, R. P., Ackrell, B. A., Sices, H., and Cecchini, G. (1993) *J. Biol. Chem.* **268**, 815–822
11. Mowery, P. C., Ackrell, B. A., and Singer, T. P. (1976) *Biochem. Biophys. Res. Commun.* **71**, 354–361
12. Mowery, P. C., Steenkamp, D. J., Ackrell, A. C., Singer, T. P., and White, G. A. (1977) *Arch. Biochem. Biophys.* **178**, 495–506
13. Degli Esposti, M. (1989) *Biochim. Biophys. Acta* **977**, 249–265
14. Broomfield, P. L. E., and Hargreaves, J. A. (1992) *Curr. Genet.* **22**, 117–121
15. Matsson, M., Ackrell, B. A. C., Cochran, B., and Hederstedt, L. (1998) *Arch. Microbiol.* **170**, 27–37
16. Ingledew, W. J., and Ohnishi, T. (1977) *Biochem. J.* **164**, 617–620
17. Salerno, J. C., and Ohnishi, T. (1980) *Biochem. J.* **192**, 769–781
18. Hägerhäll, C. (1994) *On the Structure and Function of Succinate: Quinone Oxidoreductase Using Bacillus subtilis as a Model Organism*. Ph.D. thesis, University of Lund, Lund, Sweden
19. Smirnova, I., Hägerhäll, C., Konstantinov, A., and Hederstedt, L. (1995) *FEBS Lett.* **359**, 23–26
20. Rothery, R. A., and Weiner, J. H. (1998) *Eur. J. Biochem.* **254**, 588–595
21. Hägerhäll, C., Fridén, H., Aasa, R., and Hederstedt, L. (1995) *Biochemistry* **34**, 11080–11089
22. Hägerhäll, C., Sled, V. D., Hederstedt, L., and Ohnishi, T. (1995) *Biochim. Biophys. Acta* **1229**, 356–362
23. Ruzicka, F. J., Beinert, H., Schepler, K. L., Dunham, W. R., and Sands, R. H. (1975) *Proc. Natl. Acad. Sci. U. S. A.* **72**, 2886–2890
24. Rich, P. R., Moore, A. L., Ingledew, W. J., and Bonner, W. D., Jr. (1977) *Biochim. Biophys. Acta* **462**, 501–514
25. Rich, P. R., and Bonner, W. D., Jr. (1978) *Biochim. Biophys. Acta* **504**, 345–363
26. Waldeck, A. R., Stowell, M. H., Lee, H. K., Hung, S.-C., Matsson, M., Hederstedt, L., Ackrell, B. C., and Chan, S. I. (1997) *J. Biol. Chem.* **272**, 19373–19382
27. Kunkel, T. A. (1985) *Proc. Natl. Acad. Sci. U. S. A.* **82**, 488–492
28. Kunkel, T. A., Roberts, J. D., and Zakour, R. A. (1987) *Methods Enzymol.* **154**, 367–382
29. Sanger, F., Nicklen, S., and Coulson, A. R. (1977) *Proc. Natl. Acad. Sci. U. S. A.* **74**, 5463–5467
30. Blaut, M., Whittaker, K., Valdovinos, A., Ackrell, B. A., Gunsalus, R. P., and Cecchini, G. (1989) *J. Biol. Chem.* **264**, 13599–13604
31. Cecchini, G., Thompson, C. R., Ackrell, B. A., Westenberg, D. J., Dean, N., and Gunsalus, R. P. (1986) *Proc. Natl. Acad. Sci. U. S. A.* **83**, 8898–8902
32. Werth, M. T., Cecchini, G., Manodori, A., Ackrell, B. A. C., Schröder, I., Gunsalus, R. P., and Johnson, M. K. (1990) *Proc. Natl. Acad. Sci. U. S. A.* **87**, 8965–8969
33. Dutton, P. L. (1978) *Methods Enzymol.* **54**, 411–435
34. Lowry, O. H., Rosebrough, N. J., Farr, A. L., and Randall, R. J. (1951) *J. Biol. Chem.* **193**, 265–275
35. Aasa, R., and Vänngård, T. (1975) *J. Magn. Reson.* **19**, 308–315
36. Vinogradov, A. D., Sled, V. D., Burbaev, D. S., Grivennikova, V. G., Moroz, I. A., and Ohnishi, T. (1995) *FEBS Lett.* **370**, 83–87
37. Rupp, H., Rao, K. K., Hall, D. O., and Cammack, R. (1978) *Biochim. Biophys. Acta* **537**, 255–260
38. Ohnishi, T., and Trumpower, B. L. (1980) *J. Biol. Chem.* **255**, 3278–3284
39. Xu, Y., Salerno, J. C., Wei, Y. H., and King, T. E. (1987) *Biochem. Biophys. Res. Commun.* **144**, 315–322
40. Miki, T., Yu, L., and Yu, C.-A. (1992) *Arch. Biochem. Biophys.* **293**, 61–66
41. Paddock, M. L., McPherson, P. H., Feher, G., and Okamura, Y. (1989) *Proc. Natl. Acad. Sci. U. S. A.* **87**, 6602–6606
42. Gray, K. A., Dutton, P. L., and Daldal, F. (1994) *Biochemistry* **33**, 723–733
43. Pace, C. P., and Stankovich, M. T. (1991) *Arch. Biochem. Biophys.* **287**, 97–104
44. Ishii, N., Fujii, M., Hartman, P. S., Tsuda, M., Yasuda, K., Senoo-Matsuda, N., Yanase, S., Ayusawa, D., and Suzuki, K. (1998) *Nature* **394**, 694–697
45. Papaefthymiou, V., Girerd, J.-J., Moura, I., Moura, J. J. G., and Münck, E. (1987) *J. Am. Chem. Soc.* **109**, 4703–4710
46. Crowe, B. A., Owen, P., Patil, D. S., and Cammack, R. (1983) *Eur. J. Biochem.* **137**, 191–196
47. Trumpower, B. L., and Gennis, R. B. (1994) *Annu. Rev. Biochem.* **63**, 675–716
48. Rothery, R. A., and Weiner, J. H. (1996) *Biochemistry* **35**, 3247–3257
49. Iverson, T., Luna-Chavez, C., Cecchini, G., and Rees, D. C. (1999) *Science* **284**, 1961–1966